Understanding Injection Locking in Negative-Resistance LC Oscillators Intuitively Using Nonlinear Feedback Analysis

Yayun Wan, Xiaolue Lai and Jaijeet Roychowdhury
Department of Electrical and Computer Engineering, University of Minnesota
Emails: {yayun,laixl,jr}@ece.umn.edu

Abstract— **Simple, accessible and intuitive treatments of oscillator injection locking, that at the same time maintain rigour especially with regard to nonlinearities, appear to be lacking in the literature. We present a novel analysis that incorporates all these features but uses only basic mathematical and circuit theory concepts. We develop a graphical procedure for finding the nonlinear relationship between injection amplitude and lock range that is both accurate and insightful. We also provide freely downloadable MATLAB scripts [2] implementing our analysis and graphical procedures. These scripts can be easily adapted to any negative-resistance LC oscillator and used for convenient and accurate exploration of injection locking and other properties.**

I. Introduction

Injection locking is a nonlinear phenomenon universal to all free-running oscillators. When an oscillator is perturbed by an external signal, its natural frequency can change to exactly equal (*i.e.*, lock to) the perturbing frequency, under the right circumstances. This phenomenon has been noted in virtually every physical discipline involving oscillators, from biological[1], chemical, mechanical and optical systems to electronic ones.

While unintended injection pulling/locking can be a severe problem in circuit applications, the effect has been increasingly exploited as a useful design technique. For example, in RF design, mutually injection-locked arrays of oscillators have been used to control the aperture phase of phased-array antennas [14]; in high-frequency PLL design, where the power consumption of frequency dividers is of concern, superharmonically injection-locked oscillator dividers can offer low-power alternatives [18]; in analog fiber-optic applications, injection locking is used to increase laser bandwidth, improve frequency stability and reduce noise and chirp [3], [8]; and so on [11], [15], [16], [19]. Given its ubiquity and myriad applications, it is not surprising that there has been great interest in developing analytical and computational methods for understanding the phenomenon [15], [16], [18]–[21].

An obvious means of predicting injection locking is brute-force simulation at the SPICE level. This approach, while straightforward, is far from ideal even if the goal is simply simulation (see, *e.g.*, [10]). From a design perspective, it provides little understanding of or insight into mechanisms behind injection locking. A variety of analytical approaches have been proposed for this purpose (*e.g.*, [1], [6], [9], [19]), of which Adler's classic 1946 paper [1] is possibly the best known. Adler was able, using linear concepts, to obtain formulae for injection locking in negative-resistance LC oscillators. In particular, Adler's analysis predicted that the locking range (*i.e.*, the maximum deviation of the perturbing frequency from the oscillator's natural frequency) of an injection-locked oscillator is *linearly related* to the amplitude of injection; this prediction has been confirmed for small injection levels. The validity of Adler's approach begins to falter at higher injection levels, however; measurements have shown that locking range deviates significantly from Adler's predictions as the injection strength grows. In addition, Adler's analysis did not deal satisfactorily with *circuit nonlinearity*, which plays a crucial rôle in the injection locking process. As noted recently [15], [19] and elaborated upon further in this paper, nonlinearity cannot simply be wished away as a second-order effect for oscillators; it is necessary to take it into account to obtain a proper understanding of even basic features of oscillator operation. For example, it is easily shown that amplitude-stable oscillation [5], [7] and especially injection locking [10], [16] cannot occur at all in purely linear systems.

The importance of nonlinearities in injection locking was recognized by Verma, Rategh and Lee [15], [19], who employed polynomial nonlinearities to obtain relatively complex formulae for a variety of injection locking scenarios. Such prior nonlinear analyses of injection locking have tended, however, to sacrifice to a large extent the simplicity, intuition and insight that is the chief attraction of linearized analyses like those of Adler [1] and Razavi [16].

In this work, we present a simple and intuitive analytical technique for understanding and predicting injection locking effects in negative-resistance LC oscillators. In spite of its simplicity, our technique is a fully nonlinear one that is rigorously developed in logical fashion. A key feature of our approach is that it uses only basic circuit concepts and considerably simpler mathematics than investigations such as [15], [19]), relying instead on a graphical development that provides considerable insight into the core nonlinear mechanisms responsible for injection locking. Furthermore, our approach is not limited to specific nonlinear forms (such as polynomials) but can treat any type of nonlinear negative resistance element. In the remainder of this section, we outline the flow of our approach.

We start (Section II) by addressing the issue of how to find the oscillation amplitude of a free-running negative-resistance oscillator with no external injection. We first review classic linear feedback structures and Barkhausen's criterion for oscillation [17], noting shortcomings that we proceed to address. We show how a negative-resistance LC oscillator can be interpreted as a nonlinear feedback structure. We present a simple but rigorous analysis of this nonlinear feedback structure, our only approximation being a natural one related to the Q factor of the LC tank. As part of this analysis, we explain intuitively why the tank voltage should be highly sinusoidal, while its current can be extremely distorted. We show how the amplitude of the tank voltage can be estimated using a simple graphical procedure, providing an analytical example as illustration. We also show how this procedure can be framed in equation form and solved using MATLAB, employing simple, freely-downloadable code which we provide [2].

We then proceed to analyze and understand injection locking using small modifications of the above nonlinear feedback structure (Section III). We show how the fundamental mechanism of injection locking can be understood via simple phasor diagrams, nonlinear generalizations of similar diagrams from linear analysis [1], [16]. From these phasor diagrams, we derive a simple and insightful graphical procedure, and provide MATLAB code, for predicting the nonlinear relationship between lock range and injection amplitude accurately. Finally, we show how Adler's classic result can be immediately visualized as a simple special case of our approach.

II. Nonlinear Feedback Analysis: Amplitude and Frequency of Negative-Resistance LC Oscillators

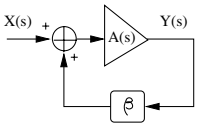

Fig. 1. Linear feedback structure.

[1]Indeed, there is speculation (*e.g.*, [12]) that complex locking phenomena within large systems of interacting oscillators is fundamental to life itself.

0-7803-9023-7/05/$20.00 ©2005 IEEE.

Oscillator operation is conventionally viewed [17] as a limiting case of the (linear) feedback amplifier shown in Fig. 1. $A(s)$ is the transfer function of an amplification block, β is a feedback factor, $X(s)$ is the input and $Y(s)$ the output; all quantities are in the Laplace domain. The input-output relationship of this feedback system is given by

$$Y(s) = \frac{A(s)}{1+\beta A(s)} X(s). \tag{1}$$

This relationship is valid for all values of β and $A(s)$, except when $\beta A(s) = -1$, *i.e.*, when the denominator of (1) vanishes, a condition called the *Barkhausen criterion* [17]. If the Barkhausen criterion is satisfied at some frequency $s = \jmath\omega_0$, the feedback amplifier is assumed to go into self-oscillation at that frequency, based on the loose reasoning that even when the input $X(s) = 0$, the output $Y(s)$ can be nonzero.

While Barkhausen's oscillation criterion has the merit of simplicity, and indeed generates insights valuable for practical oscillator design, it also raises basic questions that hint at shortcomings. If the system does oscillate, what is the output amplitude? Is the output waveform always sinusoidal? What happens if the input $X(s)$ is nonzero while Barkhausen is satisfied – can the output amplitude blow up to infinity? Such egregious implications are typically countered by noting that β or $A(s)$ are in fact nonlinear and that they actually change with the amplitude of X or Y; hence that the quantities in (1) should be interpreted in some kind of "average" sense, "over an oscillation cycle". But such notions, while certainly intuitive, have so far been of limited predictive value in design, failing to provide even qualitative insight into observed phenomena like injection locking. One of the purposes of this paper is to show that such intuition can in fact be made rigorous and predictive, while at the same time enhancing insight and understanding.

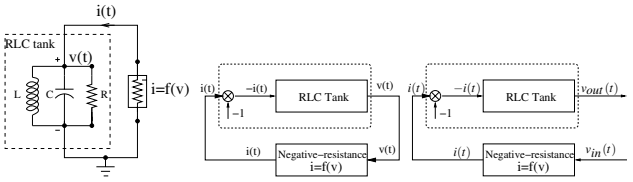

Fig. 2. Negative-resistance LC oscillator as a nonlinear feedback system.

The first step towards achieving this is to interpret negative-feedback LC oscillators, such as the one depicted in Fig. 2(a), as feedback systems similar to Fig. 1, but with the crucial difference that nonlinearity is incorporated explicitly from the start. Such a nonlinear feedback system is shown in Fig. 2(b). To appreciate the equivalence, we view the boxed LC tank circuit in Fig. 2(a) as an input-output system with input current $-i(t)$ and output voltage $v(t)$. The nonlinear resistor is also viewed as a memoryless input-output system, with input voltage $v(t)$ and output current $i(t)$ related by $i = f(v)$, where $f(\cdot)$ is a suitable negative resistance nonlinearity, to be discussed further shortly. It is these input-output blocks that are shown in the feedback structure of Fig. 2(b), together with connections implied by the nodal connections of Fig. 2(a).

Next, as shown in Fig. 2(c), we cut the feedback loop on the voltage side. (Note that cutting only the voltage side of the feedback loop is an abstraction, not easy to achieve physically by, *e.g.*, cutting the wire at the upper Fig. 2(a) — this would correspond to cutting both voltage and current sides of Fig. 2(c).). This enables us to investigate how the opened loop acts, on any $v_{\rm in}(t)$ that we apply, to produce $v_{\rm out}(t)$. For reasons that will become clear shortly, we choose to apply a sinusoid $v_{\rm in}(t) = A\cos(\omega_0 t)$.

Observe that $v_{\rm in}(t)$ is first acted upon by the memoryless nonlinear resistor to produce $i(t) = f(v_{\rm in}(t))$. Since $v_{\rm in}(t)$ is *periodic* (with period $T = \frac{2\pi}{\omega_0}$), $i(t)$ must also be periodic with the same period, regardless of what the nonlinearity $f(\cdot)$ is. Since any periodic waveform can always be expressed in Fourier series [13] (*i.e.*, in terms of DC, fundamental and higher harmonic sinusoidal components), we can express $i(t)$ as

$$i(t) = \sum_{k=-\infty}^{\infty} I_k(A) e^{\jmath k\omega_0 t}. \tag{2}$$

In (2), $I_k(A)$ are complex numbers that represent the amplitudes/phases of the harmonics of $i(t)$. We shall be concerned primarily with the fundamental harmonic component, $I_1(A)$, for reasons again to be noted later. Note that all the harmonics depend on the input amplitude A and, of course, on the nature of the nonlinearity $f(\cdot)$.

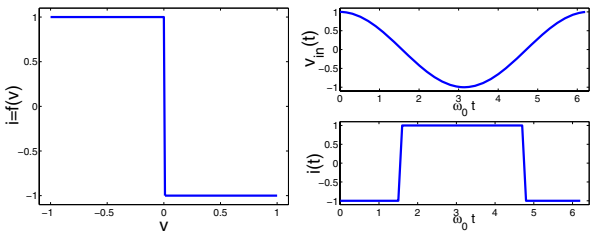

(a) plot of $i = f(v)$ (b) plots of $v_{\rm in}(t)$ (upper) and $i(t) = f(v_{\rm in}(t))$ (lower)

Fig. 3. Simple hard negative resistance nonlinearity: $f(v) = \pm 1$

We illustrate how $I_1(A)$ is related to A using a simple concrete example of a "hard" negative-resistance nonlinearity, shown in Fig. 3(a). The current through this nonlinear resistor switches abruptly between ± 1 as the voltage across it changes from negative to positive; in other words, the "resistor" behaves like a ideal current source of value ± 1, except at $v = 0$, where it has infinite negative differential resistance. (Note that such a nonlinearity is not amenable to representation using polynomials.) If a sinusoidal voltage of any nonzero amplitude A is applied across this nonlinearity, the current $i(t)$ through it is a square wave as a function of time, as shown in Fig. 3(b). The first harmonic component (*i.e.*, the fundamental) of this current has amplitude $\frac{4}{\pi}$ and a phase shift of 180° or π radians. Hence, for this nonlinearity, $I_1(A)$ can be expressed analytically as $I_1(A) = \begin{cases} \frac{2}{\pi} e^{\jmath\pi}, & A > 0 \\ 0, & A = 0. \end{cases}$. The magnitude of $I_1(A)$ is plotted vs A in

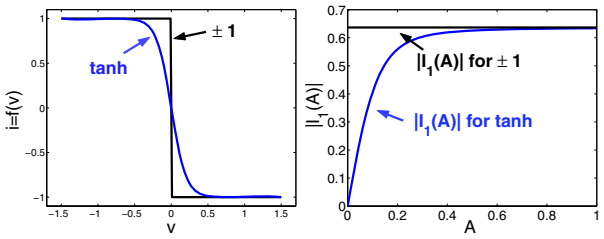

(a) (b)

Fig. 4. (a) Negative resistance. (b) $I(A)$ versus A.

Fig. 4(b) for this $f(v)$ (black line). A "softer" $\tanh(\cdot)$ nonlinearity, more representative of real nonlinear resistors encountered in practice (particularly in cross-coupled CMOS topologies), is shown by the blue line in Fig. 4(a). The plot of $|I_1(A)|$ vs A for this nonlinearity is also depicted in blue, in Fig. 4(b). Such plots of $|I_1|$ vs A can be easily generated for any nonlinear resistor using a simple MATLAB routine [2]; for many analytical nonlinearities, closed-form formulae are available as well.

We have already noted above that for the memoryless nonlinearity of Fig. 3(a), a phase shift of π is obtained from the input fundamental to the output fundamental. This fact is true for *any* nonlinear resistor with a negative differential operating characteristic. Even

more generally, it can be shown that for any nonlinearity $f(v)$, the phase of $I_1(A)$ will be either 0 or π, possibly changing from one to the other as A is changed[2].

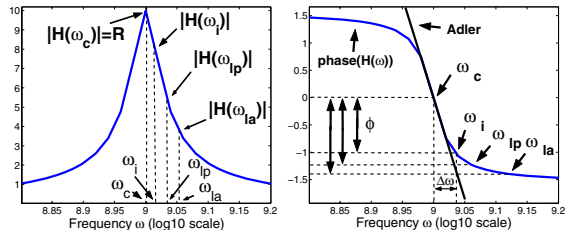

(a) (b)

Fig. 5. Open-loop magnitude (a) and phase (b) characteristics of the RLC tank.

So far, we have seen that when a sinusoidal waveform of amplitude A is applied at $v_{\text{in}}(t)$, the resulting current $i(t)$ through the memoryless negative-resistance nonlinearity features a fundamental component $I_1(A)$, with phase shift π and amplitude varying with A as shown in Fig. 4(b). The current will, in general, also feature DC and higher harmonic components, possibly very significant ones depending on how strongly nonlinear $f(v)$ is. We now consider the effect of the LC tank circuit on $i(t)$. Observe that the tank acts as a *filter* on $i(t)$ to produce $v_{\text{out}}(t)$. The filter characteristic is simply the impedance of the tank, plotted in Fig. 5. The amplitude characteristic peaks (with value R), and the phase characteristic passes rapidly through zero, at the resonant frequency $\omega_c = 1/\sqrt{LC}$. We now set the frequency of the input $v_{\text{in}}(t)$, ω_0, to equal the filter's center frequency ω_c.

The rate at which the filter's amplitude characteristic rolls off depends on the Q factor of the tank [4]; for any reasonable value of Q, the roll-off is rapid, with the amplitude characteristic becoming essentially zero at the higher harmonics of ω_0 (and exactly zero at DC). *It is for this reason that we have not been concerned with higher harmonics of* $i(t)$, since only its fundamental component survives at $v_{\text{out}}(t)$ after filtering by the LC tank. *This observation justifies our original purely sinusoidal choice of* $v_{in}(t)$. At the fundamental frequency $\omega_0 = \omega_c$, the LC tank simply scales its input fundamental component $I_1(A)$ by $-R$ (recall that the minus sign stems from reversing $i(t)$ as it enters the tank (Fig. 2(b)). This corresponds to a magnitude scaling of R and an additional phase shift of π.

We are now in a position to understand the nonlinear feedback system of Fig. 2(c) both intuitively and quantitatively. We have shown that if $v_{\text{in}}(t)$ is a sinusoid of magnitude A at the tank's resonant frequency ω_0, then $v_{\text{out}}(t)$ is also a sinusoid at the same frequency, with amplitude $2R|I_1(A)|$ and relative phase shift 2π (or equivalently, 0). To close the loop as in Fig. 2(b), we must have $v_{\text{in}}(t) = v_{\text{out}}(t)$, or

$$A = 2R|I_1(A)| \Leftrightarrow \frac{2R}{A}|I_1(A)| = 1 \Leftrightarrow \boxed{\frac{A}{2R} = |I_1(A)|}. \qquad (3)$$

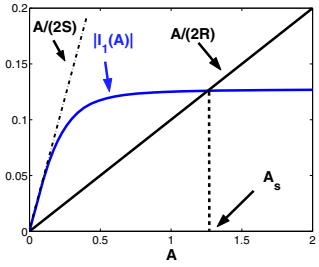

Fig. 6. Solution A_s using nonlinear feedback analysis.

Solving (3) determines the amplitude of oscillation A_s. The boxed form of (3) is particularly insightful from a graphical perspective, as shown in Fig. 6, where the left hand side $\frac{A}{2R}$ is overlaid on Fig. 4(b) as a straight line with slope $\frac{1}{2R}$. The intersection of the two traces represents the solution of (3) for the amplitude of oscillation A_s. Using Fig. 6, the effect of changes to tank or nonlinear resistor parameters on the oscillator's amplitude can be understood in an intuitive, visual manner. The solution of (3) can also be obtained via the simple MATLAB scripts provided [2].

[2]a proof of this fact is omitted for brevity.

III. Injection Locking via Nonlinear Feedback

We now consider the situation when the oscillator is perturbed by an external injection signal. Fig. 7(a) depicts how an injected voltage source modifies the circuit, while Fig. 7(b) shows the corresponding modification to the cut nonlinear feedback structure of Fig. 2(c). (Note that we could also consider current source injections; the analysis and conclusions obtained are essentially equivalent, particularly for injection frequencies close to the fundamental.) We consider a sinusoidal injection $v_i(t) = A_i\cos(\omega_i t + \phi_i)$, where ω_i is assumed close to the fundamental frequency ω_0.

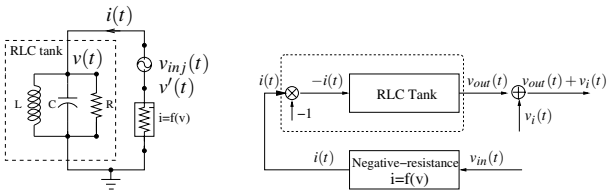

(a) into circuit (b) into feedback structure

Fig. 7. Negative-feedback LC oscillator with voltage injection

If the oscillator is injection locked, then only the injection frequency ω_i will remain and the natural frequency ω_0 will disappear. Motivated by this observation, we re-enact the nonlinear open-loop analysis of the previous section, but with the difference that the input is now taken to be $v_{\text{in}}(t) = A\cos(\omega_i t)$, *i.e.*, at the injection frequency ω_i instead of at the natural frequency $\omega_0 = \omega_c$.

Since the nonlinearity is memoryless, all conclusions about $i(t)$ and $I_1(A)$ from the previous section (*i.e.*, upto Fig. 4) remain exactly the same in spite of the frequency change. Moreover, since we have assumed that ω_i is close to ω_c (the LC tank filter's center frequency), all non-fundamental harmonics of $i(t)$ still remain far from the ω_c peak, hence are filtered out. The only change is the impact of the tank filter on the fundamental component $I_1(A)$ of $i(t)$, no longer centered exactly at the amplitude peak (or the zero phase shift point) of the filter. As a result, the fundamental component of the filtered output $v_{\text{out}}(t)$ is $H(\omega_i)I_1(A)$, where $H(\omega_i)$ now has a nonzero phase shift and an amplitude less than the peak value of R. The change in amplitude and phase is depicted pictorially in Fig. 5. The filter characteristic's amplitude at ω_i is $|H(\omega_i)| < R$ and its phase is $\phi = \angle H(\omega_i)$.

If the injection amplitude were zero, we would not be able to close the feedback loop and set $v_{\text{in}}(t) = v_{\text{out}}(t)$, since there would be some phase shift ϕ around the loop — even if the modified amplitude condition $A = 2|H(\omega_i)||I_1(A)|$ were satisfied. From this observation, the main rôle of the injection $v_{\text{i}}(t)$ immediately becomes clear: to *add to the output of the tank filter so as to restore the total loop phase shift to exactly* 2π *and the amplitude to exactly* A. This requirement for locking, that the output of the tank filter should add to the injection to exactly equal the input, is depicted pictorially using phasors in Fig. 8(b). Note that the phasor illustration captures both amplitude and phase requirements for locking and is, furthermore, completely valid regardless of how large the injection amplitude is, what the injection frequency ω_i is, or how strongly nonlinear the negative resistor is. The only assumption on which Fig. 8(b) is predicated is that all non-fundamental harmonics of $i(t)$ have been filtered out by the LC tank filter. The phasor locking diagram is easily expressed in equation form and solved using, *e.g.*, the simple MATLAB programs supplied [2]. Considerably more insight into locking and its limits is

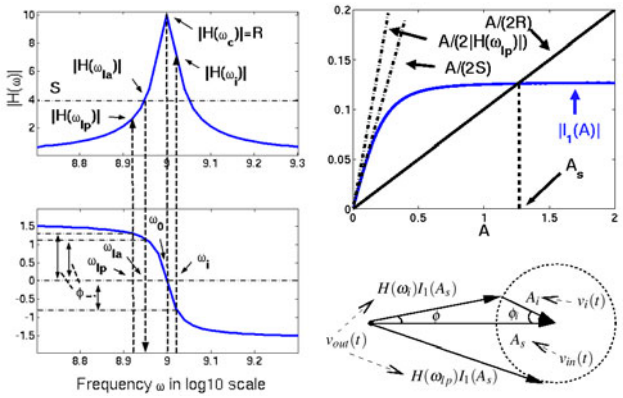

(a) (b)

Fig. 8. Phase relationship between input and output

obtained, however, by a simple graphical procedure for approximately solving these equations, which we now outline.

The lock range of an oscillator, for a given injection amplitude A_i, is usually of great design interest. The condition for locking encapsulated in Fig. 8(b) suggests a simple graphical procedure to find the lock range. The natural amplitude of oscillation of the unlocked oscillator is first found and marked as a phasor on Fig. 8(b). A circle of radius A_i is drawn, centered at the tip of the phasor, and the tangent from the origin to this circle is drawn to determine the *maximum value of* ϕ supported for injection locking. The frequency deviation ω_{lp} (from the center ω_c) for this ϕ is then read off the phase characteristic of Fig. 8(a). This frequency deviation is a phase-dominated upper limit for the lock range.

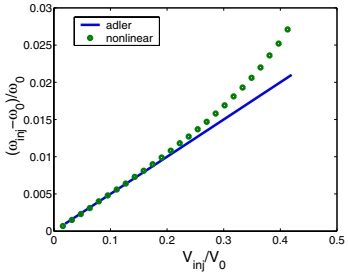

Fig. 9. Lock range: Adler vs ω_{lp}

To ascertain if ω_{lp} is indeed the real lock range, it is necessary to confirm that the amplitude gain at ω_{lp} supports oscillation. This can also be achieved in an intuitive graphical fashion, using Fig. 8(b). The straight line $\frac{A}{2R}$ is simply replaced by $\frac{A}{2|H(\omega_{lp})|}$, with a slope greater than $\frac{A}{2R}$. If the two curves still intersect, then the lock range is determined primarily by the phase and equals ω_{lp}. If there is no intersection, however, the lock range is smaller than ω_{lp}, being limited by amplitude gain constraints. This smaller lock range ω_{la} can also be estimated graphically, by first finding the maximum slope $\frac{A}{2S}$ of any straight line that supports an intersection point in Fig. 8(b). By marking off S on the vertical axis of the amplitude characteristic of Fig. 8(a) and reading off the corresponding frequency deviation, the (amplitude-limited) lock range ω_{la} can be found.

Finally, we note that the well-known result of Adler [1], that the locking range is linearly proportional to the injection A_i, is simply an (extreme) simplification of the above procedure: the phase characteristic of Fig. 5/Fig. 8(a) is simply assumed to be perfectly linear around the point of its maximum slope at ω_c, as depicted within Fig. 5(b) (the amplitude condition is not considered at all in Adler's analysis). A better estimate, still ignoring the amplitude condition, is given by the phase-limited lock range ω_{lp} as noted above. Fig. 9 compares the (over-conservative) prediction by Adler against the more accurate ω_{lp}.

IV. Summary

We have presented a rigorous, yet simple and intuitive, nonlinear analysis method for understanding and predicting injection locking in LC oscillators. We use minimal mathematics and rely largely on graphical procedures and insight instead of formulae. Our technique is easily extended to provide insight into, and quantitative calculations for, a variety of other injection related phenomena, including sub- and super-harmonic locking, multiplicative injection, *etc.*. We have provided code implementing our approach as freely-downloadable MATLAB scripts.

Acknowledgments

Roychowdhury thanks the organizers of AACD 2005 in Limerick for bringing together circuit design and CAD researchers in a relaxed and convivial atmosphere, thus fostering discussions that engendered this work. In particular, he would like to thank Michael Peter Kennedy (University College, Cork) and Peter Kinget (Columbia) for providing motivation for this work as well as pointers to the existing literature. Support from the NSF, SRC, DARPA and the University of Minnesota's Digital Technology Center is gratefully acknowledged.

References

[1] R. Adler. A study of locking phenomena in oscillators. Proceedings of the I.R.E. and Waves and Electrons, 34:351–357, June 1946.
[2] Analog System Verification Group, University of Minnesota. http://laoo.dtc.umn.edu/~jr/code/injlock/.
[3] C. Chang, L. Chrostowski, C. J. Chang-Hasnain, and W. W. Chow. Study of long-wavelength vcsel-vcsel injection locking for 2.5-gb/s transmission. IEEE Photonics Technology Letters, 14(11):1635–1637, November 2002.
[4] W. Chen. The circuits and filters handbook. CRC Press LLC, Florida, 2003.
[5] A. Demir, A. Mehrotra, and J. Roychowdhury. Phase noise in oscillators: a unifying theory and numerical methods for characterization. IEEE Trans. Ckts. Syst. – I: Fund. Th. Appl., 47:655–674, May 2000.
[6] J. Van der Pol. Forced oscillations in a circuit with nonlinear resistance. Phil. Mag., 3:65–80, January 1927.
[7] M. Farkas. Periodic Motions. Springer-Verlag, 1994.
[8] S. Kobayashi and T. Kimura. Injection locking characteristics of an algaas semiconductor laser. IEEE J. Quantum Electron., 16:915–917, September 1980.
[9] K. Kurokawa. Injection locking of microwave solid state oscillators. Proc. IEEE, 61:1386–1410, October 1973.
[10] X. Lai and J. Roychowdhury. Capturing oscillator injection locking via nonlinear phase-domain macromodels. IEEE Trans. Microwave Theory Tech., 52(9):2251–2261, September 2004.
[11] J. Lee and B. Razavi. A 40-ghz frequency divider in 0.18-μm cmos technology. IEEE Journal of Solid-State Circuits, 39(4):594–601, April 2004.
[12] N. H. Lovell, S. L. Cloherty, B. G. Celler, and S. Dokos. A gradient model of cardiac pacemaker myocytes. Progress in Biophysics and Molecular Biology, 85:301–323, 2004.
[13] A. Papoulis. Signal Analysis. McGraw-Hill, New York, 1977.
[14] R. J. Pogorzelski, P. F. Maccarini, and R. A. York. Continuum modeling of the dynamics of externally injection-locked coupled oscillator arrays. IEEE Trans. Microwave Theory Tech., 47(4):471–478, April 1999.
[15] H.R. Rategh and T.H. Lee. Superharmonic injection-locked frequency dividers. IEEE Journal of Solid-State Circuits, 34:813–821, June 1999.
[16] B. Razavi. A study of injection locking and pulling in oscillators. IEEE Journal of Solid-State Circuits, 39(9):1415–1424, September 2004.
[17] A. S. Sedra and K. C. Smith. Microelectronic Circuits. Oxford, U.K.: Oxford Univ. Press, 1991.
[18] M. Tiebout. A cmos direct injection-locked oscillator topology as high-frequency low-power frequency divider. IEEE Journal of Solid-State Circuits, 39(7):1170–1174, July 2004.
[19] S. Verma, H.R. Rategh, and T.H. Lee. A unified model for injection-locked frequency dividers. IEEE Journal of Solid-State Circuits, 38(6):1015–1027, June 2003.
[20] H. Wu and A. Hajimiri. A 19 ghz 0.5 mw 0.35 μm cmos frequency divider with shunt-peaking locking-range enhancement. In Proc. IEEE ISSCC, pages 412–413, 471, February 2001.
[21] S.-M. Wu and W.-L. Chen. A 5.8-ghz cmos vco with injection-locked frequency divider for ieee 802.11a application. In Proc. ECCTD, Cracow, Poland, September 2003.